

# A VERSATILE NEW SENSOR FOR Pu ASSAY AND INDEPENDENT MEASUREMENTS OF NEUTRONS AND GAMMA RAYS

## LA-UR-02-0542

A. P. Belian, M. C. Browne, W. Clay, W. Geist, H. Nguyen, K. Ianakiev, D. Mayo, S. Panowski, P. Russo  
Los Alamos National Laboratory / NIS-5  
P.O. Box 1663, MS E-540  
Los Alamos, NM, 87545, USA  
(505) 665-7239  
abelian@lanl.gov

### SUMMARY

A new well counter has been developed at Los Alamos National Laboratory that integrates the neutron capture medium ( $^6\text{LiF}$ ) and scintillator ( $\text{ZnS}$ ) into a thin screen, which is coupled to wavelength shifting fiber-optic ribbon. A four-sided prototype well counter has been built. It has a short neutron die-away time ( $t = 5.8 \mu\text{s}$ ), which increases its sensitivity to measurements of  $^{240}\text{Pu}$  by neutron coincidence counting. The neutron detection efficiency for this counter is 20%.

### I. INTRODUCTION

Neutron coincidence counters (NCCs) have been valuable tools for the nondestructive analysis (NDA) of special nuclear materials.<sup>1-3</sup> They measure correlated fission neutrons emitted by plutonium to determine its mass. A new NCC uses  $^6\text{Li}$  to capture neutrons in a scintillator coupled to fiber-optic ribbon. It has been developed to address measurement limitations inherent in counters utilizing  $^3\text{He}$  tubes.

Molten salt extraction (MSE) is a process in which plutonium metal plus oxidant are melted in a molten salt to extract  $^{241}\text{Am}$  that has built up from the decay of  $^{241}\text{Pu}$ . Some plutonium is also oxidized and some remains as metal in the salt residue. Safeguard-able quantities of plutonium and relatively large amounts of  $^{241}\text{Am}$  can be present in these residues. There are two sources of neutrons in Am-extraction residues: correlated spontaneous fission neutrons from isotopes of plutonium ( $^{238}\text{Pu}$ ,  $^{240}\text{Pu}$ , and  $^{242}\text{Pu}$ ), and uncorrelated ( $\alpha, n$ ) neutrons from interactions between alpha particles from actinide (primarily  $^{241}\text{Am}$ ) decay and low-Z nuclei in the salt. This counter is intended to measure the plutonium content in Am-extraction residues by neutron coincidence counting. Coincidence counting distinguishes between time-correlated neutrons and uncorrelated neutrons from ( $\alpha, n$ ) sources.

The neutron coincidence or doubles rate is related to the plutonium mass.<sup>4</sup>

Conceptually, a gate in time is opened when a neutron pulse arrives in the shift register. The "coincidence gate" width is determined by the die-away time of the detector. The neutron die-away time is the average lifetime of a neutron in the detector. Any other neutron pulse that enters the shift register during the coincidence gate is either a true (real) coincident neutron from the same spontaneous fission, or an accidental coincidence neutron from other fission events or ( $\alpha, n$ ) reactions. These are the "real plus accidental" (R+A) coincidences. The "accidental" coincidence rate (A) is determined by sampling the total neutron rate. It is the product of the totals rate (T) squared and the coincidence gate width (G):  $T^2G$ . Finally, the accidentals are subtracted from the reals plus accidentals to give the real coincidence rate:  $R=(R+A)-A$ .

### II. THE WELL COUNTER

This counter has a short die-away time ( $\tau = 5.8 \mu\text{s}$ ) relative to  $^3\text{He}$  counters ( $\tau > 20 \mu\text{s}$ ). Its coincidence gate is shorter resulting in a reduced ratio of accidental to real coincidences. This is an advantage in measurements of samples with high ( $\alpha, n$ ) neutron yields. The effect of  $\tau$  on the assay precision for residues is seen in Figure 1. The TNMC<sup>5</sup> is the thermal neutron multiplicity counter using 4-atmosphere  $^3\text{He}$  tubes, and the ENMC<sup>6</sup> is the epithermal neutron multiplicity counter using 10-atmosphere  $^3\text{He}$  tubes. Their die-away times are  $50 \mu\text{s}$  and  $22 \mu\text{s}$ , respectively. Figure 1 shows the expected uncertainty in plutonium mass as a function of  $\alpha$ , the ratio of ( $\alpha, n$ ) neutrons to spontaneous fission neutrons. As  $\alpha$  increases, a shorter die-away time is required achieve a fixed assay precision.

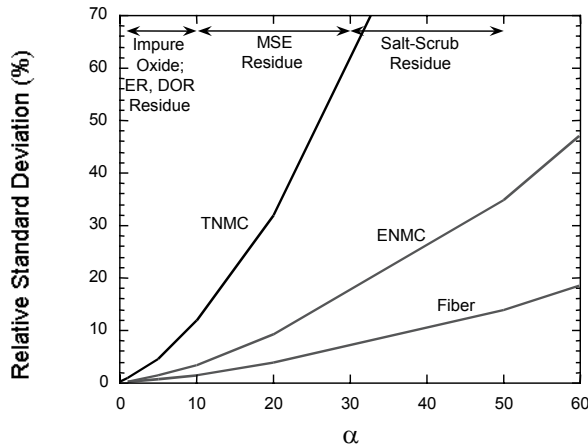
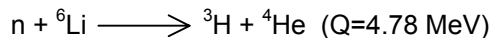


**Figure 1. Expected precision in plutonium mass vs.  $\alpha$  for three NCCs. The residue categories (labeled above) have typical  $\alpha$  ranges.**

#### A. New Sensor Construction and Physics

The sensor is made of alternating layers of neutron capture/scintillator screens and wavelength shifting (WLS) fiber-optic ribbons. The capture/scintillator screen is composed of granular  $^6\text{LiF}$  and  $\text{ZnS(Ag)}$  in a hydrogenous binder. Charged particles from the exothermic neutron-capture reaction



deposit energy in nearby  $\text{ZnS}$  granules, which scintillate blue light. The scintillation light is emitted in  $4\pi$ , absorbed in the WLS fiber optic ribbon and re-emitted in  $4\pi$  as green light. The light is transmitted to both ends of the ribbon where it is detected in photomultiplier tubes (PMTs). This kind of detector has an improved die-away time relative to  ${}^3\text{He}$ -tube detectors because the density of capture nuclei is greater and the hydrogenous moderator and capture media are more intermixed compared to  ${}^3\text{He}$  detectors.

Unlike  ${}^3\text{He}$ , scintillators are sensitive to gamma rays. However, pulse decay times (shapes) for  $\text{ZnS(Ag)}$  depend on charge density and are short for gamma rays and long for charged nuclear particles (tritons, alpha particles, etc.). Therefore, pulse-shape analysis (PSA) can differentiate gamma-ray and neutron interactions. Typical preamplifier pulse shapes for both gamma-rays and neutrons shown in Figure 2 illustrate the longer decay time for neutron interactions. Custom PSA electronics have been developed using a combination of pre-filtering and delay-line

shaping coupled with a modified time pickoff. The result is a bipolar shaped pulse with a zero crossing.

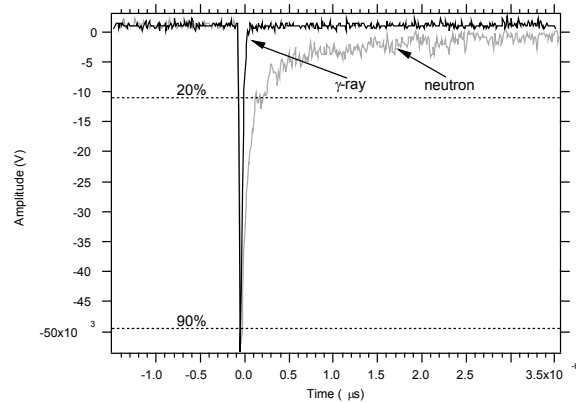


**Figure 2. Typical pulses from gamma-ray and neutron events in the detector.**

#### B. Well Counter Construction and Performance

The sensors described in the previous section have been developed into a four-sided well counter.<sup>7,8</sup> A single unfinished side of the well counter is shown in Figure 3. The completed well counter is undergoing testing and evaluation. The total counter efficiency, die-away time, and coincidence counting rate are being measured.



**Figure 3. One side of the four sided well counter. Each side is composed of three detector elements. The capture/scintillator screens, wavelength shifting fiber optic ribbon and PMTs are all visible.**

The counter is made up of 12 individual detector elements, three per side. The completed counter is shown in Figure 4. The outputs of both PMTs from an element go to one preamplifier, whose output is the input of a PSA board. Its output is a logic pulse for each neutron detected. The neutron

detection efficiency of 20% was measured using  $^{252}\text{Cf}$  placed in the center of the well.



**Figure 4.** The prototype scintillator based well counter. One can clearly see two of the four sides with the associated hardware. The sample holder is shown in the foreground, which is inserted into the middle of the counter via a hole in the top.

The neutron die-away time was also measured using  $^{252}\text{Cf}$ . The combined logic pulses from the 12 PSA boards form the input to the shift register. The neutron die-away time was measured by counting doubles versus shift-register

- 1.) pre-delay at a fixed gate width
- 2.) gate width at a fixed pre-delay.

The decay constant of an exponential curve fit to these data gives the die-away time as shown in Figure 5 and Figure 6.

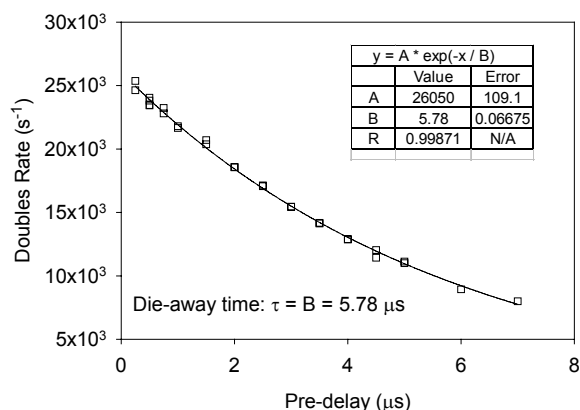


**Figure 5.** Well counter doubles rate vs. pre-delay for a fixed gate width. The B term in the exponential is the die-away time  $\tau$ .

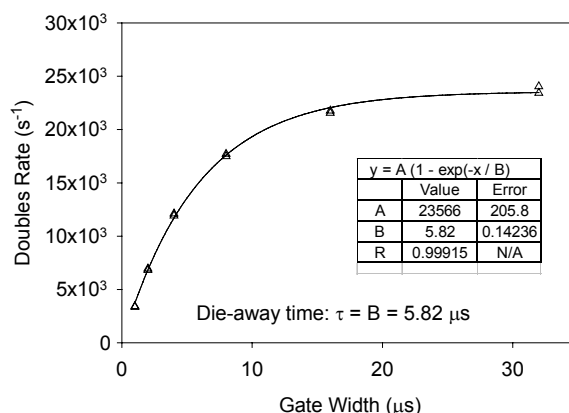


**Figure 6.** Well counter doubles rate vs. gate width for a fixed pre-delay. The B term in the exponential is the die-away time  $\tau$ .

The weighted average of the two measured die-away times gives  $\tau = 5.79 \pm 0.0037$ . This important parameter determines the optimum gate width for the shift register.

Coincidence measurements have been done with  $^{252}\text{Cf}$  and AmLi sources. Figure 7 shows the precision in the doubles rate vs. gate width for two different pre-delays. These data, measured with a  $^{252}\text{Cf}$  spontaneous fission source, illustrate a near-minimum in precision with a short (4- $\mu\text{s}$ ) gate width.

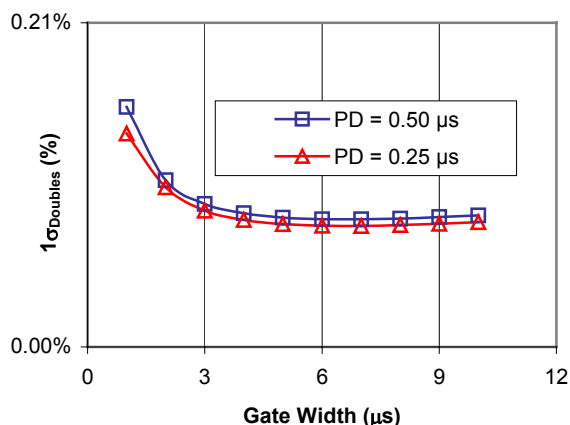


**Figure 7. Uncertainty in the <sup>252</sup>Cf doubles rate vs. the gate width for two predelay settings.**

Problems arise in coincidence measurements with AmLi sources. Neutrons from AmLi are uncorrelated in time; only one neutron is emitted per ( $\alpha, n$ ) reaction. Therefore, the doubles rate should be zero. As shown in Figure 8, there is a non-zero (negative) doubles bias.

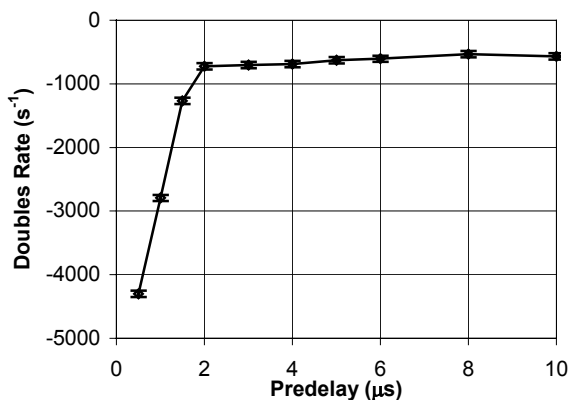


**Figure 8. The AmLi doubles rate vs. predelay with a fixed gate width of 4 μs.**

The “short-term” (predelay < 2 μs) negative bias is a dead-time effect. The PSA electronics blocks the time-to-amplitude converter (TAC) from processing pulses for ~2 μs after any pulse (gamma-ray or neutron) is processed. This causes the (R+A) rate for same-channel correlations to be low relative to the A rate, causing the negative doubles rate. Once the predelay exceeds the TAC blocking time, the

doubles rate becomes nearly constant. However, it is still negative.

Possible reasons for the “long-term” (predelay > 2 μs) negative bias are 1.) a sagging of the photomultiplier gain during the very long neutron pulse and/or 2.) pulses that pile up on the negative lobe of the shaped analog pulse. The first scenario causes some same-channel second pulses within the (R+A) gate timing to fall below the event threshold of the PSA electronics. The second situation would cause some same-channel second events within the (R+A) gate timing to fall below the event threshold. One solution is to eliminate the short component by blocking the TAC (effectively) for the entire coincidence gate width (~ 4 μs) only for neutron events. This will eliminate same-channel coincidences, causing a small loss of efficiency. However, supported by additional measurements of the totals rate in individual channels (to correct the overestimated A), it should also eliminate the short- and long-term negative doubles bias. The negative real phenomenon is rate dependent, so it should also be possible to make an empirical correction to the negative real bias based on the total neutron rate measured in each detector element.

### III. OTHER USES OF THE SENSOR

The sensor’s malleability and intrinsic position sensitivity make it an excellent candidate as a  $4\pi$ , directionally sensitive neutron and gamma-ray detector.

Timing analysis of signals from the photodetectors at the ends of the fiber bundle gives the position of the interaction along the length of the sensor. The sensors can also be shaped and fit together with an appropriate core, as in Figure 9, that prohibits radiations incident on one side of the detector from interacting on the opposite side.

Multiple directional detectors of this type can locate gamma-ray and neutron sources (independently) by triangulation. The applications include counterterrorism and nuclear smuggling.

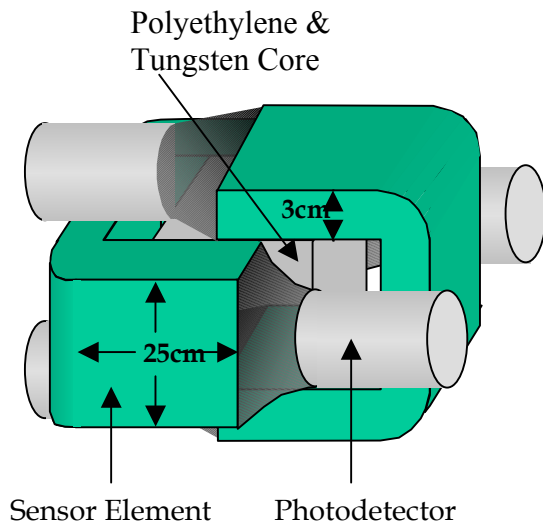


**Figure 9. Conceptual six-sided (two-element) detector. Two sensor elements surround the polyethylene and tungsten core on its six sides.**

## REFERENCES

1. N. Ennsin *et al.*, "Evaluation of Several Fast Neutron Coincidence Counter Options for Characterization of Remote-Handled TRU Waste," 7th Nondestructive Assay Waste Characterization Conference, Salt Lake City, Utah, May 23-25, 2000, Los Alamos National Laboratory document LA-UR-00-1742.
2. H.O. Menlove *et al.*, "The SuperHENC Mobile Passive Neutron Waste Measurement System for Counting Plutonium in Standard Waste Boxes," 7th Nondestructive Assay Waste Characterization Conference, Salt Lake City, Utah, May 23-25, 2000, Los Alamos National Laboratory document LA-UR-00-1687.
3. H.O. Menlove, *et al.*, "Advanced Performance Epithermal Neutron Detector for Measurement of Inventory Samples," Sixth International Conference on Facility Operation - Safeguards Interface, Jackson Hole, Wyoming, September 20-24 1999, Los Alamos National Laboratory document LA-UR-99-2861.
4. N. Ennsin, *et al.*, "Application Guide to Neutron Multiplicity Counting," Los Alamos National Laboratory report LA-13422 (1998).
5. H.O. Menlove, *et al.*, "The Design of a High Efficiency Neutron Counter for Waste Drums to Provide Optimized Sensitivity for Plutonium Assay," Los Alamos National Laboratory document LA-UR-96-4585 (1996).
6. J.E. Stewart, *et al.*, "Epithermal Neutron Multiplicity Counter (ENMC): Current Developments and Applications," Los Alamos National Laboratory document LA-UR-00-3137 (2000).
7. W.H. Geist, *et al.*, "Development of a Neutron Multiplicity Counter Utilizing Scintillator based Detectors," submitted to *Nuclear Instruments and Methods*, Los Alamos National Laboratory document LA-UR-01-4397 (2001).
8. M.C. Browne, *et al.*, "Prototype Neutron-Capture Counter for Fast-Coincidence Assay of Plutonium in Residues," Los Alamos National Laboratory document LA-UR-01-2164, (2001).